Optical trapping and binding of particles in an optofluidic stable Fabry–Pérot resonator with single-sided injection

Noha Ali Aboulela Gaber, Maurine Malak, Frédéric Marty, Dan E Angelescu, Elodie Richalot, Tarik Bourouina

▶ **To cite this version:**

Noha Ali Aboulela Gaber, Maurine Malak, Frédéric Marty, Dan E Angelescu, Elodie Richalot, et al.. Optical trapping and binding of particles in an optofluidic stable Fabry–Pérot resonator with single-sided injection. Lab on a Chip, 2014, 14 (13), pp.2259-2265. 10.1039/c3lc51438b . hal-01438420

HAL Id: hal-01438420
https://hal.science/hal-01438420

Submitted on 31 Jan 2017

HAL is a multi-disciplinary open access archive for the deposit and dissemination of scientific research documents, whether they are published or not. The documents may come from teaching and research institutions in France or abroad, or from public or private research centers.

L'archive ouverte pluridisciplinaire **HAL**, est destinée au dépôt et à la diffusion de documents scientifiques de niveau recherche, publiés ou non, émanant des établissements d'enseignement et de recherche français ou étrangers, des laboratoires publics ou privés.

Journal Name

Dynamic Article Links►

Cite this: DOI: 10.1039/c0xx00000x

www.rsc.org/xxxxxx

PAPER

Optical Trapping and Binding of Particles in an Optofluidic Stable Fabry–Pérot Resonator with Single-Sided Injection

Noha Gaber,*[a]Maurine Malak[b], Frédéric Marty[a], Dan E. Angelescu[a], Elodie Richalot[a], Tarik Bourouina[a]

Received (in XXX, XXX) Xth XXXXXXXXX 20XX, Accepted Xth XXXXXXXXX 20XX

DOI: 10.1039/b000000x

In this article, micro particles are manipulated inside an optofluidic Fabry–Pérot cylindrical cavity embedding a fluidic capillary tube, taking advantage of field enhancement and multiple reflections within the optically-resonant cavity. This enables trapping of suspendedparticles with single-side injection of light and with lowoptical power. A Hermite-Gaussian standing wave is developed inside the cavity, forming trapping spots at the locations of the electromagnetic field maxima with strong intensity gradient. The particles get arranged in a pattern related to the mechanism affecting them:either optical trapping and/or optical binding. This is proven to eventually translate into either an axial one dimensional (1D) particle array or a cluster of particles, respectively. Numerical simulations are performed to model the field distributions inside the cavity allowing a behavioral understanding of the phenomena involved in each case.

1. Introduction

Optical trapping is grasping huge attention due to its important applications in the handling and analysis of micro and nano particles as well as their sorting.[1]To this end, the majority ofexperimental setups adopt free space tightly focused light beams to achieve the gradient in the electromagnetic field needed for obtaining optical tweezers; but most often than not, the optical setup is off-chip and requires rather high optical power, typically hundreds of milliwatts or even few watts.[1-4]

To overcome the bulky, free space universaloptical tweezers, the use of optical integrated structures and optical resonators is being extensively investigatedto achieve on-chip, low power and compact size optical traps; which led to the development of different configurations to achieve localization control and/or simple manipulation. To name some of these on-chip optical trapping modules: evanescent fields from waveguides and Whispering Gallery Mode resonators,in the form of ring resonators,[5] disks,[6] or spheres[7] are used to propel particles along the light propagating path.Multimode-interference (MMI) structures[8] and photonic crystals[9] are used to trap particles at specific locations. Among all these techniques, none has the full three-dimensional (3D) handling capabilities provided by the conventional optical tweezers.So-far, the best miniaturized configuration regarding simplicity, and low optical power in tradeoffs with trapping and manipulationperformance is probably the counter-propagating dual-beam trap thatis formed by two single-mode optical fibers.[10,11]This kind of traphas the advantage of confining the objects placed between the two opposite waves coming from the two fibers without the need of focusing components, because the generated opposed optical forces trap the particles. A standing wave is formed due to interference between these two waves traveling in opposite directions,[12]but in some cases – if needed – this stationary wave can be avoided by slightly misaligning the fibers to simplify the system analysis.[13]Although the dual-beam trap is simple, it requires splitting the light path to provide double-side injection of light and it also strongly depends on the mutual fiber alignment. Using a Fabry–Pérot (FP) cavity avoids these issues by providing the two counter-propagating waves in the form of a standing waveresulting from the multiple reflections of the light –injected from a single side only–by both cavities' mirrors. This way, particles can be trapped and aligned axially, due to thehighest light intensity in the antinodes of the formed standing wave.[14]Also, the use of a stable, high quality resonator achieves field enhancement inside the cavityproportionally to its finesse (ratio of optical quality factor over mode order), thus allowing the operation of trapping with lowlevels of input light power. Furthermore,the stable resonanceprovides the additional advantage of field confinement inside the cavity and forms well-focused field pattern that provides high intensity gradientsfor efficient trappingof particles. However, under some conditions of the particles size and/or concentration, the optically illuminated particles exhibit their own mutually interacting scattered fields, leading to their self-arrangement into clusters, or what is called 'optical matter'.[15]This interesting phenomenon of light-matter interaction is referred as 'optical binding'.[13, 16]The behavior of either optical binding or hybrid effect of combined optical trapping and binding mechanisms appear as dependent on how particles disturb the field due to their size and/or distribution as will be shown in the experimental section and the discussion.

Up to our knowledge, this is the first useof on-chipresonant FP cavity in trapping micrometer particles. This is particularly difficult since the stabilitywith a Gaussian beam inputis not easily achievable on-chip: it requires very challenging micro-fabrication

of spherical micro-mirrors facing each-other. Our group could overcome this problem by adopting a combination of cylindrically-curved surfaces to obtain stable, high quality factor FP resonators with a cavity length extendingup to 280 µm,[17] thus providing enough space for injecting fluid samples through capillary tubes, as demonstrated in this work, wherethe tubes also performin theopticalconfinement.

It is worth-mentioning that short, unstable FP cavities were occasionally reported for being used mainly for refractometry of single particles but not for theirtrapping.[18]On the other hand, bulky, off-chip FP cavities (of spherical mirrors) are also used in quantum electrodynamics (QED) studies toinvestigate the interaction between atoms and the strong cavity field, but this is out of scope of our study.[19-21]Also, it is good to mention that while optical trapping involves both the quantum and electromagnetic nature of light, dielectrophoretic manipulation[22] can be also seen somehow as a close mechanism but it requires applying much lower-frequency electric fields through electrodes.Also beside the electromagnetic trapping techniques, there are acoustical,[23,24] and hydro-dynamical[25] techniques that also allow very efficient micro particles trapping. When one deals with biological particles, on-chip cell trapping is important for a variety of applications,[26,27] such as on-chip cell culture, cell enrichment, as well as cell sorting. It might be also important for identifying waterborne bacteria. To this end, the use of optical trapping rather than other trapping methods provides the additional capability of achieving optical spectroscopy analysis of the trapped cell.[28]Further on-chip implementation inside a resonant cavity provides *in situ* capabilities for such optical spectroscopy analysis. Of course one needs to pay special attention to the viability of the biological sample exposed to light, which can be preserved at low optical powers, especially when choosing suitable working wavelengths in the near infrared region; for example Escherichia coli bacterial cells show minimum damage at wavelengths 970 nm and 830 nm,[29] while microalgal cells are preserved when exposed in the 886-1064 nm range.[30] The study of biological particles is not considered for the moment in this paper, whose focus is intended to provide a better understanding of the optical trapping and optical binding mechanisms of micro-particles inside an optofluidic resonant cavity. Of special interest are the particles whose dimensions are in the order of 0.5-2 µm, corresponding not only to the smallest bacterial cell's dimensions, but also to the wavelength of light being used in most optical trapping experiments. Larger size particles, up to 6 µm are also considered in order to evaluate the size effects.In this report, an optofluidic stable Fabry–Pérot cavity is used to study the behavior of micro-particles suspended in liquid environment when exposed to a resonant light field. The phenomena of optical trapping and optical binding have been observed experimentally inside such devices and explained upon behavioral analysis with the help of numerical simulations.

2. Experimental Setup

Ouroptofluidic structure consists of a FP resonator formed by two cylindrical Silicon/air Bragg mirrors with cylindrical lens in-between. The latter is actually formed by a capillary microtube holding a fluid with suspended particles. A schematic view of the device is illustrated in Figure 1; the cylindrical mirrors achieve lateral confinement of the light field, while the tube with the liquid inside –acting as a cylindrical lens- achieves a vertical confinement, leading to field focusing and strong optical gradient, essential for efficient optical trapping.

Figure 2 photos the setup of the silicon chip with the capillary tube, connected to external larger tubing. The chip is placed on a positioner with 2 degrees of freedom (DOF) between the Input/Output fibers, which are manipulated using 5-DOFpositioners. The inset shows a cavity with the cylindrical Bragg mirrors, the microtube in-between, and the placement of the injecting/collecting lensed fibers. The chip contains many FP cavities with different design dimensions to offer different quality factor/free spectral range tradeoffs.

For our experiments, we selecteda FP cavity having a physical length of 280 μm formed by cylindrical silicon-air Bragg mirrors, each consists of 3 curved silicon layers with radius of curvature of 140 μm and thickness of 3.67 μm for the silicon wall and 3.48 μm for the air gap (the equivalence of an odd multiple of quarter wavelengthin each medium).

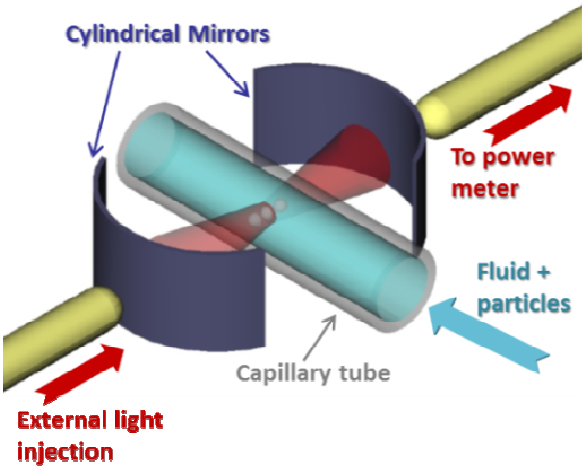

Fig. 1 Schematic diagram of the cylindrical Fabry–Pérot cavity with the capillary micro tube inside, also acting as a cylindrical lens, and the injecting/collecting lensed fiber pair.

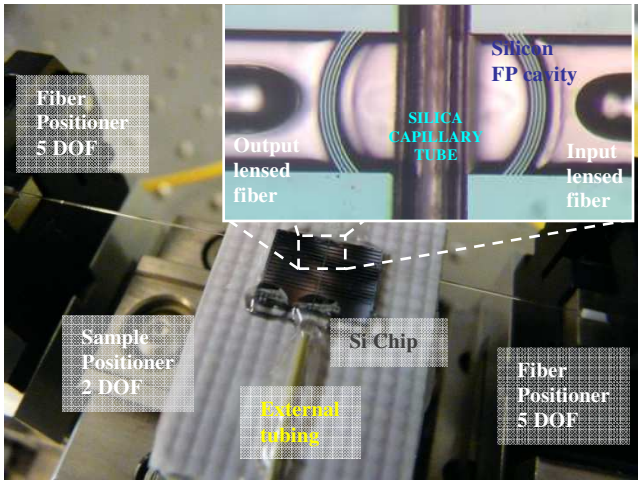

Fig. 2 Photo of the setup of the silicon chip with the capillary tube connected to the injection tubing, and the I/O fibers on their positioners. The inset is a zoom of the cavity indicating the placement of the lensed fiber pair, one being used for light injection and the other for recording the spectral transmission response.

A fused silica microtube with outer diameter of 128.1±1.2 μm and inner diameter of 75.3±1.2μm (Polymicro Technologies TSP075150) is placed between the mirrors and is connected with an external larger diameter tube to allow injecting the fluid. The experiments are done by inserting the liquid with a suspension of spherical polystyrene beads (Polysciences) inside the tube using a syringe, then stopping the flow to provide static conditions for the experiments. Variable sizes of beads were used, ranging between 1 μm and 6 μm diameter. The liquid surrounding the particles was either DI water or acetone. The water may cause some losses due to its absorption at this wavelength range, but it was found to be affordable due to the short optical path across the microtube diameter. On the other hand, when using acetone, the polystyrene beads shouldn't be stored in it for long periods to avoid their dissolution. Un-polarized light in the near infrared region was injected into the cavity from a laser source tunable within the C and L bands, with power range from 4 mW to 30 mW, using single mode lensed fiber with a beam waist diameter of 18 μm .To determine the correct resonance wavelength that should be used for trapping, the spectral response was recorded first -as shown in Fig. 3 - by performing a wavelength scan and recording the transmission by a second lensed fiber connected to a power meter. After this initial step, the input light for the trapping experiments was fixed at the selected resonance wavelength chosen with a reasonably high quality factor (in the order of 1000) and high transmitted power level. Note in Fig.3 that beside the fundamental resonance peaks, there are other side peaks corresponds to other modes supported by these types of resonators.[31] The system is observed by a stereo microscope and the results are recorded by a C-MountCMOS camera attached to the microscope.

3. Experimental Results

A few seconds after injecting the laser light set at 30 mW into the above-described optofluidic cavity, the microspheres get arranged in certain configuration depending on the particles size and concentration. Figure 4 (a) shows 1 μmdiameter polystyrene beads in DI-water (concentration about $6.68\times10^{7} particles/cm^{3}$) aligned along the cavity axis when a 1592.4 nm wavelength beam –corresponding to cavity resonance – is injected. The quality

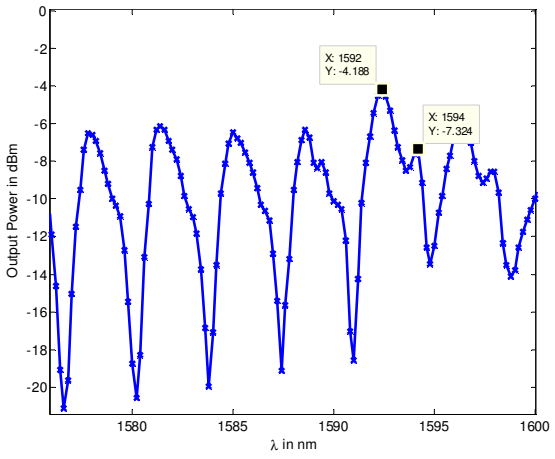

Fig. 3 The spectral response of the cavity with the microtube filled with deionized water and suspension of *1* μm diameter polystyrene beads.

factorat this peak is about 1090, and the finesse is about 7. The time taken by the beads to be completely arranged is about 1 min. Detailed process of the beads getting arranged in a line, then being almost instantaneouslydismissed after switching the laser off, is recorded in Movie 1 of the ESI. As shown in Figure 4 (b), this one-dimensional line arrangement could also be obtained by injecting light at a wavelength of 1594.2 nm(corresponding to the side peak indicated in Figure 3).Probably due to the lensing effect of the cylindrical capillary tube, the image of the particle array is deformed horizontally. Therefore, the spacing between the particles looks not uniform as indicated by the arrows in the zoomed area inside the inset. This behavior of particles lining-up will be explained in the discussion section.

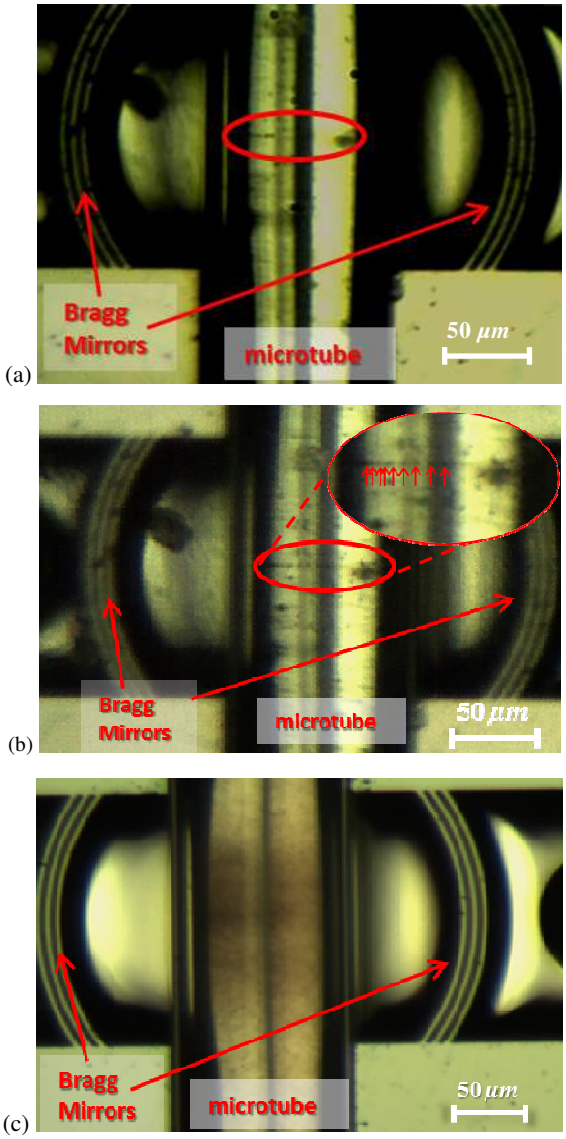

Fig. 4 Polystyrene beads diluted in water inside the optofluidic cavity, (a) 1D array of 1 μm diameter beads is formed along the cavity axis at the fundamental resonance wavelength of 1592.4 nm. (b) similar behavior observed at the side peak wavelength of 1594.2 nm. The inset is a zoom of the particles' array with their apparent positions indicated by arrows.(c) relates to concentrated 0.5 μm diameter beads which gather in the vicinity of the cavity axial region after time of 20 min, at source optical power of 10 mW.

On the other hand, if the particles' concentration is high, the observed behavior is different: the particles accumulate in the axial region but not necessarily forming an array as in the former situation. This behavior is shown in Figure 4 (c); the 0.5 μm diameter polystyrene beads in DI-water with initial concentration of about $6.27\times10^{10} particles/cm^3$ have higher concentration within the region illuminated by the light inside the cavity other than the outside regions after 20 *min* from switching the light source on, at power of 10 *mW*. The same behavior was obtained also with 1 μmdiameter polystyrene beads in DI-water or acetone. An important note is that this behavior happens even if the wavelength injected to the cavity is off-resonance, while the previously described alignment necessarily requires operation at resonance. The behavior of larger bead sizes is apparently similar to the latter phenomenon. As seen in Figure 5, the 3 μm diameter microspheres (concentration of about $8.36\times10^{7} particles/cm^3$) tend to gather slowly into a cluster over a longer time. The initially randomly dispersed beads inside the cavity, shown in Figure 5 at time 0, needed more than 10 *min* to accumulate together and reach a bound assembly. This clustering behavior has been observed for beads with diameters of 2, 3, 4.5 and 6 μm in DI water or acetone. Generally, larger beads require longer times to accumulate.The recovery time after cutting the light off in this case is also high, in the order of minutes depending on the particles' size and the degree of their clustering; while it was in the order of seconds, in the case of the accumulation of the smaller beads of 0.5 and 1 μm diameter. It also increases if their initial concentration is higher. This is predictable as this behavior is related to the natural diffusion process of the particles. For the trapped pattern, the 1D array of the separated 1μm diameter beads almost instantaneous diffused after switching the laser off, as shown in Movie 1 of the ESI; so it can be claimed to be in the order of fractions of a second. One can conclude that the diffusion time of the particles was roughly proportional to their size, as predicted by the Stokes-Einstein relation, when the trapped particle density was low. When clusters of particles were formed, inter-particle forces increased the stability of aggregates, which became slow to disperse (several minutes) particularly when the larger particles were involved.It is worth-noting that the low optical power levels involved in these experiments are not sufficient to trap particles moving in a flowing stream. In order to not increase difficulties, the beads are moving in a static liquid, naturally moving only due to the temperature-related Brownian motion that is counteracted by the applied optical forces within the resonant cavity.

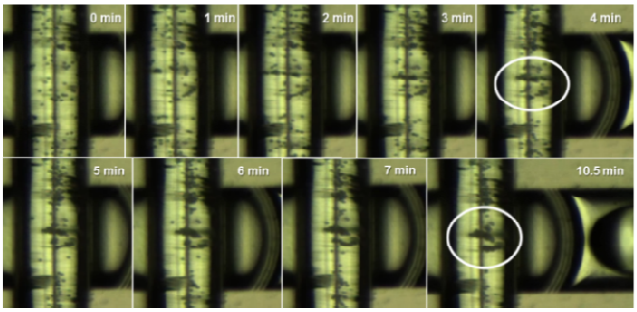

Fig. 5 The accumulation of 3 μm diameter polystyrene beads inside the cavity over time of about 10 *min*.

4. Discussion

4.1 Numerical simulations

Since the diameter of our microspheres (d) is comparable to the wavelength (λ), it doesn't fall into any of the regions in which the calculations could be simplified, which are Ray Optics Regime ($d>>\lambda$) and Rayleigh Regime ($d<<\lambda$).Then, careful numerical finite element method (FEM) simulations need to be performed. We used the ANSOFT High Frequency Structural Simulator (HFSS) software, to get an idea about the field distribution inside the cavity. Since the behavior of beads suspension depends on the relative wavelength/particles relation, actual sizes of microspheres should be simulated; the cavity and the capillary dimensionsas well asthe beam waist size should be also at least in the same order of magnitude as the actual ones. To accomplish the simulation task with the limited computational resources, we adopted what may be called 2D simulations. A cavity with a small height (a slice) is modeled, and symmetry conditions are imposed as boundary conditions on the parallel planes delimiting the cavity height to mirror the structure.The height of the slice is taken as 0.1 μm. The planar dimensions are taken as the cavity actual size presented in section 2; but to limit the number of unknown and thus the memory requirement, the cylindrical mirrors are modeled as one single layer having the smallest possible thickness that is one quarter of wavelength in silicon. The light source was chosen as a TE-polarized Gaussian beam located at a distance from the input side equivalent to the working distance of the lensed fiber used in the experiments.Despite the few differences between the model and the actualphysical case, this simulation may give an idea about the lateral field distribution at different resonance conditions, but first the spectral responses should be calculated to determine the frequencies correspond to (on-) or (off-) resonance for these simulated structures.Theyhave been obtained by performing a frequency sweep and plotting the integrated power on a sheet at the output area versus the frequency (which can be scaled into wavelength in post processing). This output power is then normalized to the input power to obtain the spectral transmission for the cases where the capillary tube is filled with water without any particles,with a single polystyrene bead of 1μm diameter, and with a single polystyrene bead of 3μm diameter, leading to determining the resonance wavelengths in each case.It is worth mentioning that the simulations presented in this paper are only for the purpose of a qualitative study of the field spatial distribution when introducing a particle of a given size inside the resonant cavity. Such simulations required simplifying the actual geometry of the resonant cavity, leading to the small discreapency between the experimental values of the resonance wavelengths and those obtained in these simulations

Figure 6 represents the field inside the cavity filled with water only.We can observe spots of high electric field intensity along the cavity axis at the resonance wavelength of λ = 1545.76 *nm*(Figure 6(a)). Away from the resonance -at λ = 1546.7*nm*as shown in Figure 6(b)- the electric field values are much less and hence no trapping is expected in this case, since those spots providing the strong intensity gradient are not available here. But still, the electric field is non-zero inside the cavity, which may lead to the scattering forces responsible of the optical

binding.Now in the case of microspheres present in water, theresonance wavelengths are slightly shifted due to the longer optical path along the cavity since the polystyrene particle has higher refractive index of 1.6 than water whose refractive index is 1.32. More importantly, the field distribution isalso altered. If a polystyrene bead of 3μm diameter is introduced near the axial line, the resonance wavelength will shift to λ = 1545.64 *nm* and the field disturbance is so severe that we have no more trapping spots as shown in Figure 7 (a), which plots the field distribution at the new resonance wavelength. Also the field intensity can be noticed to be lower due to the scattering loss. On the contrary, if a bead with 1μm diameter is introduced at the same location, the field spots are still preserved despite the scattering due to the small particle and hence the bead can in this case, continue traveling to its minimum energy position corresponding to the field intensity maxima, as shown in Figure 7 (b) that plots the field distribution at the resonance wavelength corresponds to this case that is λ = 1545.8*nm*. This may explain why only the small beads with 1μm diameter could be trapped and arranged along the axial line (Figure 4 (a) and (b)) while the larger beads could not (Figure 5).

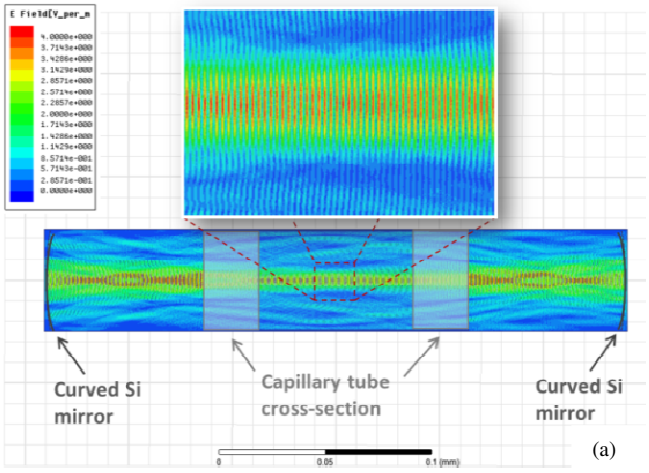

Fig. 6 Numerical simulations of the electric fielddistribution inside the cylindrical FP cavity with the tube filled with water (a) at the resonance wavelength of the modeled 2D structure: λ = 1545.76*nm*. (b)Off-resonance: λ =1546.7*nm*.The insets are a zoom for the area inside the microtube region. The high intensity interference spots can be observed at the resonance wavelength only, but not formed off-resonance.

4.2 Phenomenological Analysis

As we have seen, both experimental and simulated behaviors depend on particles size as they affect the field distribution in different manners. Generally, besides the Brownian motion of the particles, one may consider two components of the optical force governing the particles arrangement: (i) the optical trapping gradient force resulting from the non-perturbed cavity field and(ii) the additional perturbation force due to light re-scattered by the particles. The particles final configuration depends on whether stable states can be achieved or not and is probably based on the relative weight between the above-mentioned two components of the optical force, resulting indifferent equilibrium positions.[12]

In our case, we believe that the optical trapping - which is a light-induced force that traps dielectric particles at the maximum of the light intensity - is responsible for the lateral alignment (perpendicular to the cavity axis) and the localization of the 1 μm diameter microspheres along the axial line.

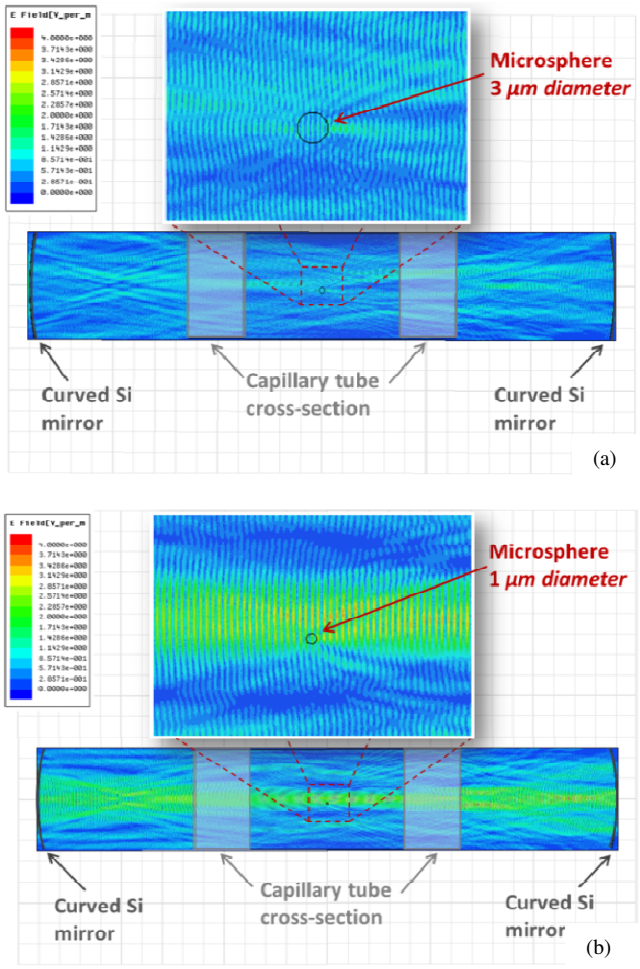

Fig. 7 Numerical simulations of the electric field within the cylindrical FP cavity enclosing the tube filled with water and a polystyrene microsphere (a) with 3μm diameter at the resonance wavelength of the modeled 2D structure: λ = 1545.64*nm*. (b) with 1μm diameter at the resonance wavelength of the modeled 2D structure: λ = 1545.8*nm*. The insets are a zoom for the area inside the microtube region. The high intensity spots are preserved in the small microsphere case, but the large microsphere significantly disturbs the field tapestry, hindering the formation of the high intensity trapping sports.

This is the effect of the lateral intensity gradient of the field spots of the standing wave maxima that can be preserved even in the presence of some particles, but with low concentrations. For the longitudinal (axial) positioning, there may be more complex behavior: the particles' locations result from the balancing of two mechanisms, the first is the axial optical gradient force.This part gets along with the term 'optical trapping' although it is a partial effect. The second mechanism is the multi-particle interacting optical force due to multiple scattering of the light from the microspheres along the axis, which is known as the longitudinal binding.[32, 33]In our case, it is not considered completely due to optical binding –although it is well established that this multiple scattering mechanism can bind dielectric microspheres into an ordered 1D array even in a counter propagating wave system where their mutual interference is avoided, and hence no standing wave maxima[13]. The reason behind our statement is that this phenomenon doesn't happen at off-resonance conditions; which infers that the existence of an external standing wave is essential, so it only happens at wavelengths corresponding to the cavities' resonance peaks whether the fundamental modes or side modes are selected. The exact analysis of these mechanisms requires proper definition of the particles positions and interspacing in the chain; but this couldn't be achieved due to the poor quality of the available images.

Now concerning the second phenomenon of particles' clustering or accumulation, it happens thanks to the optical binding for larger beads and even with the 1 μm diameter beads at high concentrations, where the existence of the particles disturbs the field trapping configuration significantly. Such arrangement is not necessarily initiated by optical traps dictated by externally imposed field gradient. The mere presence of the objects in the area illuminated by the optical field exhibits its own field tapestry and even any new particle added in its vicinity, leads to a new spatial distribution.[12]That is why the binding could happen even if we work off-resonance.

5. Conclusion

We demonstrated a novel method for low power particle localization inside a symmetric optofluidicFP using single side injection of light and taking advantage of both field confinement and field enhancement. We studied the phenomena of microspheres' optical trapping and binding. Small micro beads of 1 μm diameter at low concentration get arranged in a 1D array along the cavity axis due to hybrid effect of optical trapping of the field gradient and longitudinal binding induced by multi-particle scattering. Under certain conditions, the optical binding leads either to form certain patterns of particles or to their accumulation even if no optical traps exist in advance or where they get disturbed by the existence of the microspheres. Numerical simulations have been performed to aid the understanding of the field distributions and hence the optical behavior in each reported case.

Notes and references

[a] *Université Paris-Est, ESYCOM EA2552, UPEMLV ESIEE Paris CNAM, Noisy-le-Grand, F-93162 France; E-mail:noha.gaber@esiee.fr*

[b] *Ecole Polytechnique Fédérale de Lausanne EPFL, Institut de Microtechnique, Neuchâtel, CH-2000 Switzerland*

1 P. Jákl, T. Čižmár, M. Šerý, and P. Zemánek, *Appl. Phys. Lett*., 2008, **92**, 161110.
2 C. Sun, Y. Huang, P. C. Cheng, H. Liu and B. Lin, *J. Opt. Soc. Am. B*, 2001, **18**, 1483.
3 D. G. Grier, *Nature*, 2003, **424**, 810.
4 A. Ashkin and J. M. Dziedzic, *Appl. Phys. Lett*., 1974, **24**, 586.
5 S. Lin, E. Schonbrun, and K. Crozier, *Nano Lett*., 2010, **10**, 2408.
6 M. Rosenblit, Y. Japha, P. Horak, and R. Folman, *Phys. Rev. A*, 2006, **73**, 063805.
7 S. Arnold, D. Keng et al., *Opt. Express*, 2009, **17**, 6230.
8 T. Lei and A. W. Poon, *Opt. Express*, 2013, **21**, 1520.
9 N. Descharmes, U. P. Dharanipathy, Z. Diao, M. Tonin, and R. Houdre, *Phys. Rev. Lett.*, 2013, **110**, 123601.
10 A. Constable, Jinha Kim, J. Mervis, F. Zarinetchi, and M. Prentiss, *Opt. Lett*.,1993, **18**, 1867.
11 C.-W. Lai, S.-K. Hsiung, Y.-Q. Chen, A. Chiou, and G.-B. Lee, *J. Microelectromech. Syst.*, 2008, **17**, 548.
12 O. Brzobohaty, V. Karasek, M. Siler, J. Trojek, and P. Zemanek,*Opt. Express*, 2011,**19**, 19613.
13 S. Wolfgang, F. Manfred, B.Stefan, and R.-M. Monika,*J. Opt. Soc. Am. B*, 2003,**20**, 1568.
14 P. Zemanek, A. Jonas, P. Jakl, M. Sery, J. Jezek, and M. Liska, *Opt. Commun.*, 2003,**220**, 401.
15 M. M. Burns, J.-M. Fournier, and J. A. Golovchenko, *Science*, 1990,**249**, 749.
16 M. M. Burns, J.-M. Fournier, and J. A. Golovchenko, *Phys. Rev. Lett*., 1989, **63**, 1233.
17 M. Malak, N. Pavy, F. Marty, Y.-A. Peter, A. Q. Liu,and T. Bourouina, *Appl. Phys. Lett.*, 2011,**98**, 211113.
18 L. K. Chin, A. Q. Liu, et al., *Appl. Phys. Lett.,* 2007, **91**, 243901.
19 J. Ye, C. J. Hood, T. Lynn, H. Mabuchi, D. W. Vernooy, and H. Jeff Kimble, *IEEE Trans. Instrum. Meas*., 1999, **48**, 608.
20 T. Ray, A. Sharma, S. Jyothi, and S. A. Rangwala, *Phys. Rev. A*, 2013, **87**, 033832.
21 H. J. Kimble, *Phys. Scr.*, 1998**, T76**, 127.
22 K. Ahn, C. Kerbage, T. P. Hunt, R. M. Westervelt, D. R. Link, and D. A. Weitz, *Appl. Phys. Lett*., 2006, **88**, 24104.
23 B. Hammarstrom, M. Evander, H. Barbeau, M. Bruzelius, J. Larsson, T. Laurel, and J. Nilsson, *Lab Chip*, 2010, **10**, 2251.
24 Y. Chen, S. Li, Y. Gu, P. Li, X. Ding, L. Wang, J. P. McCoy, S. J. Levinee, and T. J. Huang, *Lab Chip*, 2014,**14**, 924.
25 M. Tanyeri, and C. M. Schroeder, *Nano Lett*., 2013, **13**, 2357.
26 H. B. Xin, Y.Y. Li, X. S. Liu, B. J. Li, *Nano Lett*., 2013, **13**, 3408.
27 B.H. Blehm, T.A. Schroer, K.M. Trybus, Y.R. Chemla, P.R. Selvin, PNAS, 2013, **10**, 3381.
28 L. B. Kong, P. F. Zhang, G. W. Wang, P. Setlow, and Y. Q. Li, *Nature Protocols,* 2011, **6**, 625.
29 K. C. Neuman, E. H. Chadd, G. F. Liou, K. Bergman, and S. M. Block, *Biophys. J*., 1999, **77**, 2856.
30 Z. Pilat, J. Jezek, M. Sery, M. Trtilek, L. Nedbal, P. Zemanek, *J. Photochem. Photobiol. B,* 2013, **121**, 27.
31 M. Malak, N. Gaber, F. Marty, N. Pavy, E. Richalot, and T. Bourouina, *Opt. Express,* 2013, **21**, 2378.
32 Zhi Hong Hang, Jack Ng, and C. T. Chan, *Phys. Rev. A*, 2008, **77**, 063838.
33 V. Karasek, T. Cizmar, O. Brzobohaty, and P. Zemanek, Phys. Rev. Lett., 2008, 101, 143601.